

# Spontaneous motion of a camphor particle with a three-mode modification from a circle

Hiroyuki Kitahata\*

*Department of Physics, Graduate School of Science, Chiba University, Chiba 263-8522, Japan*

Yuki Koyano†

*Department of Physics, Graduate School of Science, Tohoku University, Sendai 980-8578, Japan*

(Dated: December 21, 2024)

Spontaneous motion of a camphor particle with a slight modification from a circle is investigated. The effect of the shape on the motion is discussed using the perturbation method. The results predict that a camphor particle with a three-mode modification from a circle moves in the direction of a corner for the smaller particle, while it moves in the direction of a side for the larger particle. The numerical simulation results well reproduce the theoretical prediction. The present study will help the understanding on the effect of the particle shape on the spontaneous motion.

## I. INTRODUCTION

The motion of living organisms has attracted interest of researchers on wide varieties of natural and social sciences. Physicists have been studying on the mechanism of the motion of living organisms such as bacteria, bird flocks, and fish schools. From a standpoint of physics, living organisms can drive themselves by dissipating free energy under nonequilibrium conditions. In this sense, self-propelled particles are one of the important examples for nonequilibrium systems. Therefore, it is also important and interesting to investigate the characteristics of self-propelled particles designated by physico-chemical systems, in which we can easily change or control the experimental parameters. There have been a lot of experimental and theoretical studies on self-propelled particles and their collective behaviors [1–5].

In considering the motion of such self-propelled particles, the symmetric properties are important in general. For example, the correlation between the cell shape and its migration direction was reported [6]. Ohta and Ohkuma have developed a theoretical framework only considering the symmetric properties [2, 7]. Their model has been further improved and adapted to a lot of kinds of systems [8, 9]. However, Ohta-Ohkuma model only suggests minimum criteria on the possible coupling between variables, and it is necessary to discuss the actual systems to determine the coupling constants.

A camphor-water system is a useful experimental system to investigate the coupling between the shape and the self-propulsion since we can design the shape of the particle. This system has been intensively studied as a good example of the self-propelled particle, where a camphor particle exhibits a spontaneous motion owing to the surface tension gradient generated by itself [10–18]. A camphor particle releases camphor molecules to the water surface, which make surface concentration field

around the particle. The surface tension gradient owing to the surface concentration field generates the force and torque working on the camphor particle. The camphor particle shape is therefore an important factor to determine the characteristics of the spontaneous motion because the concentration field is affected by the camphor particle shape. Moreover, the particle shape also affects the force and torque, since they result from the surface tension at the particle periphery. Actually, there have been several studies focusing on the effect of its shape or deformation [13, 19–23]. We also previously investigated the motion of an elliptic camphor particle as the most fundamental modification from a circle [24, 25]. In our previous study, we performed a perturbation approach and calculated the change in the bifurcation point at which the rest state is destabilized and spontaneous motion appears. The analysis predicts that an elliptic camphor particle is propelled in the direction of its minor axis, and experimental and numerical results support the theoretical prediction. The perturbation approach was adopted to a camphor particle with a higher-mode modification from a circle, but we could not obtain nontrivial results [18]. That is to say, the previous approach is only applicable to a camphor particle with a two-mode modification from a circle. To discuss a camphor particle with a generic shape, we should develop analytical methods.

In the present study, we analyze a camphor particle motion in a more generic way than in the previous work; We calculate the force and torque when the camphor particle is moving at a constant velocity. As a result, we obtain nontrivial results for the camphor particle with the three-mode modification from a circle. First, we introduce a theoretical model for the camphor particle motion in Sec. II. In Sec. III, we consider the case with a circular camphor particle and then a camphor particle with the  $n$ -mode modification from a circle. We especially focus the two- and three-mode modification. Then, we check the validity of the analysis using numerical calculation in Sec. IV, and we discuss the correspondence to the actual systems and the application to the other systems in

\* kitahata@chiba-u.jp

† koyano@cmpt.phys.tohoku.ac.jp

Sec. V.

The present results on the correlation between the motion and shape will be of value in discussing the generic correlation between the motion and dynamic deformation; for example in a droplet system driven by the surface tension gradient [5, 26–31]. The present model is fundamental and therefore it can also be adopted to the other model systems with chemotactic behaviors [32, 33].

## II. THEORETICAL MODEL

The theoretical model used here is the same as the one used in the previous work [14–18, 24, 25]. The model is composed of a reaction-diffusion equation for the dynamics of the surface concentration of camphor molecules,  $u(\mathbf{r}, t)$  for  $\mathbf{r} = (x, y) \in \mathbb{R}^2$ , and the Newtonian equations for the dynamics of the center position  $\mathbf{r}_c$  and characteristic angle  $\theta_c$  of the camphor particle.

As for the dynamics of the surface concentration of camphor molecules,  $u(\mathbf{r}, t)$ , we have

$$\frac{\partial u}{\partial t} = D \nabla^2 u - au + \frac{S_0}{A} \Theta(\mathbf{r}; \mathbf{r}_c, \theta_c), \quad (1)$$

where the first, second, and third terms of the right-hand side correspond to the diffusion at the water surface, the evaporation to the air, and the release of camphor molecules from the particle, respectively.  $D$  is the diffusion coefficient, and  $a$  is the evaporation rate of camphor molecules from the surface. It should be noted that the transport by Marangoni effect due to the surface tension gradient is assumed to be included in the diffusion term [34–36], where  $D$  should be an “effective” diffusion coefficient. Here,  $S_0$  is the amount of camphor molecules released to the water surface per unit time, and  $A$  is the basal area of the camphor particle. The release term is explicitly described as

$$\Theta(\mathbf{r}; \mathbf{r}_c, \theta_c) = \begin{cases} 1, & \mathbf{r} \in \Omega(\mathbf{r}_c, \theta_c), \\ 0, & \mathbf{r} \notin \Omega(\mathbf{r}_c, \theta_c). \end{cases} \quad (2)$$

Here,  $\Omega(\mathbf{r}_c, \theta_c)$  is the region in  $\mathbb{R}^2$ , which corresponds to the inside of the camphor particle, and it is described as

$$\Omega(\mathbf{r}_c, \theta_c) = \{\mathbf{r} \mid \mathcal{R}(-\theta_c)(\mathbf{r} - \mathbf{r}_c) \in \Omega_0\}, \quad (3)$$

where  $\Omega_0$  corresponds to the region of the camphor particle when  $\mathbf{r}_c = \mathbf{0}$  and  $\theta_c = 0$ .  $\mathcal{R}(\theta)$  is the two-dimensional rotation matrix,

$$\mathcal{R}(\theta) = \begin{pmatrix} \cos \theta & -\sin \theta \\ \sin \theta & \cos \theta \end{pmatrix}. \quad (4)$$

It is noted that the area of  $\Omega_0$  is equal to  $A$ .

As for the dynamics of the center position  $\mathbf{r}_c$  and the characteristic angle  $\theta_c$  of the camphor particle, we have

$$m \frac{d^2 \mathbf{r}_c}{dt^2} = -\eta_t \frac{d\mathbf{r}_c}{dt} + \mathbf{F}, \quad (5)$$

$$I \frac{d^2 \theta_c}{dt^2} = -\eta_r \frac{d\theta_c}{dt} + N, \quad (6)$$

where  $m$ ,  $I$ ,  $\eta_t$ , and  $\eta_r$  represent the mass, the moment of inertia, the resistance coefficient for translational motion, and the one for rotational motion, respectively. The force  $\mathbf{F}$  and torque  $N$  are given as

$$\begin{aligned} \mathbf{F} &= \int_{\partial\Omega(\mathbf{r}_c, \theta_c)} \gamma(u(\mathbf{r}')) \mathbf{n}(\mathbf{r}') d\ell' \\ &= \iint_{\Omega(\mathbf{r}_c, \theta_c)} \nabla' \gamma(u(\mathbf{r}')) dA', \end{aligned} \quad (7)$$

$$\begin{aligned} N &= \int_{\partial\Omega(\mathbf{r}_c, \theta_c)} \mathbf{r}' \times \gamma(u(\mathbf{r}')) \mathbf{n}(\mathbf{r}') d\ell' \\ &= \iint_{\Omega(\mathbf{r}_c, \theta_c)} \mathbf{r}' \times \nabla' \gamma(u(\mathbf{r}')) dA', \end{aligned} \quad (8)$$

where  $d\ell'$  is the arc element along the periphery  $\partial\Omega(\mathbf{r}_c, \theta_c)$  of the region  $\Omega(\mathbf{r}_c, \theta_c)$ ,  $\mathbf{n}(\mathbf{r})$  is a unit normal vector directing outward of the particle at  $\mathbf{r}$ ,  $dA'$  is the area element on  $\Omega(\mathbf{r}_c, \theta_c)$ , and  $\nabla'$  is the vector differential operator with respect to  $\mathbf{r}'$ . The operator “ $\times$ ” denotes  $\mathbf{a} \times \mathbf{b} = a_1 b_2 - a_2 b_1$  for  $\mathbf{a} = a_1 \mathbf{e}_x + a_2 \mathbf{e}_y$  and  $\mathbf{b} = b_1 \mathbf{e}_x + b_2 \mathbf{e}_y$ , where  $\mathbf{e}_x$  and  $\mathbf{e}_y$  are the unit vectors in  $x$ - and  $y$ -directions. The detailed calculations for Eqs. (7) and (8) are shown in Appendix A.  $\gamma(u)$  is a function for the surface tension depending on the camphor molecule concentration. It is known that  $\gamma(u)$  is a decreasing function [37] and, for simplicity, we assume a linear relationship,

$$\gamma(u) = \gamma_0 - \Gamma u, \quad (9)$$

where  $\gamma_0$  is the surface tension of pure water, and  $\Gamma$  is a positive constant.

These equations are transformed into the dimensionless form in which length, time, concentration, and force units are  $\sqrt{D/a}$ ,  $1/a$ ,  $S_0/a$ , and  $\Gamma S_0/\sqrt{aD}$ , respectively. The dimensionless form used for the theoretical analysis is as follows:

$$\frac{\partial u}{\partial t} = \nabla^2 u - u + \Theta(\mathbf{r}; \mathbf{r}_c, \theta_c), \quad (10)$$

$$\Theta(\mathbf{r}; \mathbf{r}_c, \theta_c) = \begin{cases} 1, & \mathbf{r} \in \Omega(\mathbf{r}_c, \theta_c), \\ 0, & \mathbf{r} \notin \Omega(\mathbf{r}_c, \theta_c), \end{cases} \quad (11)$$

$$\Omega(\mathbf{r}_c, \theta_c) = \{\mathbf{r} \mid \mathcal{R}(-\theta_c)(\mathbf{r} - \mathbf{r}_c) \in \Omega_0\}, \quad (12)$$

$$m \frac{d^2 \mathbf{r}_c}{dt^2} = -\eta_t \frac{d\mathbf{r}_c}{dt} + \mathbf{F}, \quad (13)$$

$$I \frac{d^2 \theta_c}{dt^2} = -\eta_r \frac{d\theta_c}{dt} + N, \quad (14)$$

$$\begin{aligned}\mathbf{F} &= - \int_{\partial\Omega(\mathbf{r}_c, \theta_c)} u(\mathbf{r}') \mathbf{n}(\mathbf{r}') d\ell' \\ &= - \iint_{\Omega(\mathbf{r}_c, \theta_c)} \nabla' u(\mathbf{r}') dA',\end{aligned}\quad (15)$$

$$\begin{aligned}N &= - \int_{\partial\Omega(\mathbf{r}_c, \theta_c)} \mathbf{r}' \times u(\mathbf{r}') \mathbf{n}(\mathbf{r}') d\ell' \\ &= - \iint_{\Omega(\mathbf{r}_c, \theta_c)} \mathbf{r}' \times \nabla' u(\mathbf{r}') dA'.\end{aligned}\quad (16)$$

Here, we consider the case that the camphor particle shape for  $\mathbf{r}_c = \mathbf{0}$  and  $\theta_c = 0$  is denoted as

$$r = R(1 + \epsilon f(\theta)), \quad (17)$$

in the two-dimensional polar coordinates, where  $\epsilon$  is an infinitesimally small parameter. In other words,  $\Omega_0$  is represented as

$$\Omega_0 = \{\mathbf{r}(r, \theta) \mid r \leq R(1 + \epsilon f(\theta))\}. \quad (18)$$

As for the explicit form of  $f(\theta)$ , we consider a sinusoidal function with wave number  $n$ ,

$$f(\theta) = \cos n\theta, \quad (19)$$

where  $n \in \mathbb{N}$  and  $n \geq 2$ .

### III. THEORETICAL ANALYSIS

#### A. Perturbation methods

In our analysis, we adopt the perturbation methods with regard to the two infinitesimally small parameters: the modification amplitude from a circular shape  $\epsilon$  and the translational speed  $\delta$  [24, 25]. By considering the degree of freedom for  $\theta_c$ , we can set the  $x$ -axis to meet the direction of translational velocity of the camphor particle without losing generality, and we consider the co-moving frame with the camphor particle. The position of the center of mass of the camphor particle is set to the origin. In the co-moving frame, whose velocity in the laboratory frame is  $\delta \mathbf{e}_x$ , Eq. (10) is transformed into

$$\frac{\partial u}{\partial t} - \delta \mathbf{e}_x \cdot \nabla u = \nabla^2 u - u + \frac{1}{A} \Theta(\mathbf{r}; \mathbf{0}, \theta_c). \quad (20)$$

Here, we calculate the steady-state concentration  $u$ , which satisfies

$$-\delta \mathbf{e}_x \cdot \nabla u = \nabla^2 u - u + \frac{1}{A} \Theta(\mathbf{r}; \mathbf{0}, \theta_c). \quad (21)$$

The steady-state concentration field  $u$  is expanded with regard to the parameters  $\delta$  and  $\epsilon$  as

$$u = \sum_{i=0}^{\infty} \sum_{j=0}^{\infty} \delta^i \epsilon^j u_{i,j}. \quad (22)$$

By substituting Eq. (22) in Eq. (20), we obtain

$$0 = \sum_{j=0}^{\infty} \epsilon^j [\nabla^2 u_{0,j} - u_{0,j}] + \frac{1}{A} \Theta(\mathbf{r}; \mathbf{0}, \theta_c), \quad (23)$$

for the order of  $\delta^0$  and

$$-\sum_{j=0}^{\infty} \epsilon^j \mathbf{e}_x \cdot \nabla u_{i-1,j} = \sum_{j=0}^{\infty} \epsilon^j [\nabla^2 u_{i,j} - u_{i,j}], \quad (24)$$

for the order of  $\delta^i$  ( $i \geq 1$ ).

Considering that  $\Theta(\mathbf{r}; \mathbf{0}, \theta_c)$  has a discontinuity at the boundary of  $\Omega(\mathbf{0}, \theta_c)$ , explicitly described in the polar coordinates as

$$\begin{aligned}r &= R[1 + \epsilon F(\theta)] \\ &= R[1 + \epsilon f(\theta - \theta_c)] \\ &= R[1 + \epsilon \cos n(\theta - \theta_c)],\end{aligned}\quad (25)$$

the steady-state concentration fields  $u$  are obtained separately in the regions inside and outside of  $\Omega(\mathbf{0}, \theta_c)$ , which are denoted as  $u^{(i)}$  and  $u^{(o)}$ , respectively. Here, it should be noted that  $\theta_c$  has  $(2\pi/n)$ -periodicity. The continuity conditions between  $u^{(i)}$  and  $u^{(o)}$  are required;  $u$  should be  $C^1$ -class, because the discontinuity of  $\Theta(\mathbf{r}; \mathbf{0}, \theta_c)$  in Eq. (23) should be compensated by  $\nabla^2 u$ , and therefore the second derivative of  $u$  should have discontinuity. The continuity conditions are explicitly expressed as

$$u^{(i)}(R(1 + \epsilon F(\theta)), \theta) = u^{(o)}(R(1 + \epsilon F(\theta)), \theta), \quad (26)$$

and

$$\left. \frac{\partial u^{(i)}}{\partial r} \right|_{r=R(1+\epsilon F(\theta))} = \left. \frac{\partial u^{(o)}}{\partial r} \right|_{r=R(1+\epsilon F(\theta))}. \quad (27)$$

By describing  $u^{(i)}$  and  $u^{(o)}$  by the expansion as

$$u^{(i)} = \sum_{i=0}^{\infty} \sum_{j=0}^{\infty} \delta^i \epsilon^j u_{i,j}^{(i)}, \quad (28)$$

$$u^{(o)} = \sum_{i=0}^{\infty} \sum_{j=0}^{\infty} \delta^i \epsilon^j u_{i,j}^{(o)}, \quad (29)$$

these conditions are expressed as

$$u_{i,0}^{(i)}(R, \theta) = u_{i,0}^{(o)}(R, \theta), \quad (30)$$

$$\left. \frac{\partial u_{i,0}^{(i)}}{\partial r} \right|_{r=R} = \left. \frac{\partial u_{i,0}^{(o)}}{\partial r} \right|_{r=R}, \quad (31)$$

for the order of  $\epsilon^0 \delta^i$  ( $i \geq 0$ ), and

$$\begin{aligned}& \sum_{k=0}^{\nu} \frac{1}{k!} [RF(\theta)]^k \left. \frac{\partial^k u_{i,\nu-k}^{(i)}}{\partial r^k} \right|_{r=R} \\ &= \sum_{k=0}^{\nu} \frac{1}{k!} [RF(\theta)]^k \left. \frac{\partial^k u_{i,\nu-k}^{(o)}}{\partial r^k} \right|_{r=R},\end{aligned}\quad (32)$$

$$\begin{aligned} & \sum_{k=0}^{\nu} \frac{1}{k!} [RF(\theta)]^k \left. \frac{\partial^{k+1} u_{i,\nu-k}^{(i)}}{\partial r^{k+1}} \right|_{r=R} \\ &= \sum_{k=0}^{\nu} \frac{1}{k!} [RF(\theta)]^k \left. \frac{\partial^{k+1} u_{i,\nu-k}^{(o)}}{\partial r^{k+1}} \right|_{r=R}, \end{aligned} \quad (33)$$

for the order of  $\epsilon^\nu \delta^i$  ( $\nu \geq 1, i \geq 0$ ). In the present study, we consider the terms up to  $\delta^3$  and  $\epsilon^1$ .

It should be noted that the area  $A$  of  $\Omega_0$  is obtained as

$$A = \pi R^2 \left( 1 + \frac{1}{2} \epsilon^2 \right), \quad (34)$$

for the shape in Eq. (25) ( $n \geq 2$ ). Here, the term proportional to  $\epsilon^2$  can be neglected since we only consider the concentration up to the order of  $\epsilon$ .

### B. Circular camphor particle

First, we consider the case with no modification from a circle. This corresponds to the concentration field  $u_{i,0}$ .  $u_{0,0}$  is obtained in the polar coordinates [24, 25] as

$$u_{0,0}^{(i)} = \frac{1}{\pi R^2} [1 - R\mathcal{K}_1(R) \mathcal{I}_0(r)], \quad (35)$$

$$u_{0,0}^{(o)} = \frac{1}{\pi R^2} [R\mathcal{I}_1(R) \mathcal{K}_0(r)], \quad (36)$$

where  $\mathcal{I}_n(\cdot)$  and  $\mathcal{K}_n(\cdot)$  are the modified Bessel functions of first and second kinds with the order of  $n$ , respectively. The steady-state concentration field is obtained by solving  $u_{i,0}$  successively. The calculation leads

$$u_{1,0}^{(i)} = \frac{1}{\pi R^2} \frac{R}{2} [r\mathcal{K}_1(R) \mathcal{I}_0(r) - R\mathcal{K}_2(R) \mathcal{I}_1(r)] \cos \theta, \quad (37)$$

$$u_{1,0}^{(o)} = \frac{1}{\pi R^2} \frac{R}{2} [-r\mathcal{I}_1(R) \mathcal{K}_0(r) + R\mathcal{I}_2(R) \mathcal{K}_1(r)] \cos \theta, \quad (38)$$

$$\begin{aligned} u_{2,0}^{(i)} &= \frac{1}{\pi R^2} \frac{R^2}{32} [r^2 (\mathcal{K}_0(R) \mathcal{I}_0(r) - \mathcal{K}_2(R) \mathcal{I}_2(r)) \\ &\quad - 2(R\mathcal{K}_1(R) \mathcal{I}_0(r) - r\mathcal{K}_0(R) \mathcal{I}_1(r))] \\ &\quad + \frac{1}{\pi R^2} \frac{R^2}{64} [2r^2 (\mathcal{K}_0(R) \mathcal{I}_0(r) - \mathcal{K}_2(R) \mathcal{I}_2(r)) \\ &\quad - rR (\mathcal{K}_1(R) \mathcal{I}_1(r) - \mathcal{K}_3(R) \mathcal{I}_3(r))] \cos 2\theta, \end{aligned} \quad (39)$$

$$\begin{aligned} u_{2,0}^{(o)} &= \frac{1}{\pi R^2} \frac{R^2}{32} [r^2 (\mathcal{I}_0(R) \mathcal{K}_0(r) - \mathcal{I}_2(R) \mathcal{K}_2(r)) \\ &\quad + 2(R\mathcal{I}_1(R) \mathcal{K}_0(r) - r\mathcal{I}_0(R) \mathcal{K}_1(r))] \\ &\quad + \frac{1}{\pi R^2} \frac{R^2}{64} [2r^2 (\mathcal{I}_0(R) \mathcal{K}_0(r) - \mathcal{I}_2(R) \mathcal{K}_2(r)) \\ &\quad - rR (\mathcal{I}_1(R) \mathcal{K}_1(r) - \mathcal{I}_3(R) \mathcal{K}_3(r))] \cos 2\theta, \end{aligned} \quad (40)$$

$$\begin{aligned} u_{3,0}^{(i)} &= \frac{1}{\pi R^2} \frac{R^2}{128} [r(R^2 + r^2)(\mathcal{K}_2(R) \mathcal{I}_2(r) - \mathcal{K}_0(R) \mathcal{I}_0(r)) \\ &\quad + 4r(R\mathcal{K}_1(R) \mathcal{I}_0(r) - r\mathcal{K}_0(R) \mathcal{I}_1(r))] \cos \theta \\ &\quad + \frac{1}{\pi R^2} \frac{R^2}{1152} [-3r^3 (\mathcal{K}_0(R) \mathcal{I}_0(r) - \mathcal{K}_2(R) \mathcal{I}_2(r)) \\ &\quad + 3r^2 R (\mathcal{K}_1(R) \mathcal{I}_1(r) - \mathcal{K}_3(R) \mathcal{I}_3(r)) \\ &\quad - rR^2 (\mathcal{K}_2(R) \mathcal{I}_2(r) - \mathcal{K}_4(R) \mathcal{I}_4(r))] \cos 3\theta, \end{aligned} \quad (41)$$

$$\begin{aligned} u_{3,0}^{(o)} &= \frac{1}{\pi R^2} \frac{R^2}{128} [r(R^2 + r^2)(\mathcal{I}_2(R) \mathcal{K}_2(r) - \mathcal{I}_0(R) \mathcal{K}_0(r)) \\ &\quad - 4r(R\mathcal{I}_1(R) \mathcal{K}_0(r) - r\mathcal{I}_0(R) \mathcal{K}_1(r))] \cos \theta \\ &\quad + \frac{1}{\pi R^2} \frac{R^2}{1152} [-3r^3 (\mathcal{I}_0(R) \mathcal{K}_0(r) - \mathcal{I}_2(R) \mathcal{K}_2(r)) \\ &\quad + 3r^2 R (\mathcal{I}_1(R) \mathcal{K}_1(r) - \mathcal{I}_3(R) \mathcal{K}_3(r)) \\ &\quad - rR^2 (\mathcal{I}_2(R) \mathcal{K}_2(r) - \mathcal{I}_4(R) \mathcal{K}_4(r))] \cos 3\theta. \end{aligned} \quad (42)$$

Using these descriptions, the force and torque in Eqs. (15) and (16) are calculated as

$$\mathbf{F} = [f_{1,0}\delta - f_{3,0}\delta^3] \mathbf{e}_x, \quad (43)$$

$$N = 0, \quad (44)$$

where

$$f_{1,0} = \frac{R^2}{4} [\mathcal{I}_0(R) \mathcal{K}_0(R) - \mathcal{I}_2(R) \mathcal{K}_2(R)], \quad (45)$$

$$\begin{aligned} f_{3,0} &= \frac{R^4}{32} \left[ -\mathcal{I}_0(R) \mathcal{K}_0(R) + \frac{2}{R^2} \mathcal{I}_1(R) \mathcal{K}_1(R) \right. \\ &\quad \left. + \mathcal{I}_2(R) \mathcal{K}_2(R) \right]. \end{aligned} \quad (46)$$

Here  $f_{1,0} > 0$  and  $f_{3,0} > 0$  for  $\forall R > 0$ .

These results suggest that a circular camphor particle moves if  $\eta_t < f_{1,0}$  and that it stops if  $\eta_t > f_{1,0}$ . Considering  $f_{3,0} > 0$ , this can be considered as a supercritical pitchfork bifurcation or drift bifurcation in dynamical systems. These results are the same as the ones shown in the previous work [18, 24, 25].

### C. Camphor particle with the $n$ -mode shape

In the case for a camphor particle with the  $n$ -mode modification from a circle as shown in Eq. (25), the expanded concentrations can be explicitly given as

$$u_{0,1}^{(i)} = \frac{1}{\pi R^2} [R^2 \mathcal{K}_n(R) \mathcal{I}_n(r)] \cos n(\theta - \theta_c), \quad (47)$$

$$u_{0,1}^{(o)} = \frac{1}{\pi R^2} [R^2 \mathcal{I}_n(R) \mathcal{K}_n(r)] \cos n(\theta - \theta_c), \quad (48)$$

$$\begin{aligned}
u_{1,1}^{(i)} = & \frac{1}{\pi R^2} \frac{R^2}{4} [-r\mathcal{K}_n(R)\mathcal{I}_n(r) + R\mathcal{K}_{n-1}(R)\mathcal{I}_{n-1}(r)] \\
& \times \cos((n-1)\theta - n\theta_c) \\
& + \frac{1}{\pi R^2} \frac{R^2}{4} [-r\mathcal{K}_n(R)\mathcal{I}_n(r) + R\mathcal{K}_{n+1}(R)\mathcal{I}_{n+1}(r)] \\
& \times \cos((n+1)\theta - n\theta_c), \tag{49}
\end{aligned}$$

$$\begin{aligned}
u_{1,1}^{(o)} = & \frac{1}{\pi R^2} \frac{R^2}{4} [-r\mathcal{I}_n(R)\mathcal{K}_n(r) + R\mathcal{I}_{n-1}(R)\mathcal{K}_{n-1}(r)] \\
& \times \cos((n-1)\theta - n\theta_c) \\
& + \frac{1}{\pi R^2} \frac{R^2}{4} [-r\mathcal{I}_n(R)\mathcal{K}_n(r) + R\mathcal{I}_{n+1}(R)\mathcal{K}_{n+1}(r)] \\
& \times \cos((n+1)\theta - n\theta_c), \tag{50}
\end{aligned}$$

$$\begin{aligned}
u_{2,1}^{(i)} = & \frac{1}{\pi R^2} \frac{R^2}{32} [R^2\mathcal{K}_{n-2}(R)\mathcal{I}_{n-2}(r) \\
& - 2rR\mathcal{K}_{n-1}(R)\mathcal{I}_{n-1}(r) \\
& + r^2\mathcal{K}_n(R)\mathcal{I}_n(r)] \cos((n-2)\theta - n\theta_c) \\
& + \frac{1}{\pi R^2} \frac{R^2}{16} \left[ -\frac{n+1}{n}rR\mathcal{K}_{n-1}(R)\mathcal{I}_{n-1}(r) \right. \\
& + (r^2 + R^2)\mathcal{K}_n(R)\mathcal{I}_n(r) \\
& \left. - \frac{n-1}{n}rR\mathcal{K}_{n+1}(R)\mathcal{I}_{n+1}(r) \right] \cos n(\theta - \theta_c) \\
& + \frac{1}{\pi R^2} \frac{R^2}{32} [r^2\mathcal{K}_n(R)\mathcal{I}_n(r) \\
& - 2rR\mathcal{K}_{n+1}(R)\mathcal{I}_{n+1}(r) \\
& + R^2\mathcal{K}_{n+2}(R)\mathcal{I}_{n+2}(r)] \cos((n+2)\theta - n\theta_c), \tag{51}
\end{aligned}$$

$$\begin{aligned}
u_{2,1}^{(o)} = & \frac{1}{\pi R^2} \frac{R^2}{32} [R^2\mathcal{I}_{n-2}(R)\mathcal{K}_{n-2}(r) \\
& - 2rR\mathcal{I}_{n-1}(R)\mathcal{K}_{n-1}(r) \\
& + r^2\mathcal{I}_n(R)\mathcal{K}_n(r)] \cos((n-2)\theta - n\theta_c) \\
& + \frac{1}{\pi R^2} \frac{R^2}{16} \left[ -\frac{n+1}{n}rR\mathcal{I}_{n-1}(R)\mathcal{K}_{n-1}(r) \right. \\
& + (r^2 + R^2)\mathcal{I}_n(R)\mathcal{K}_n(r) \\
& \left. - \frac{n-1}{n}rR\mathcal{I}_{n+1}(R)\mathcal{K}_{n+1}(r) \right] \cos n(\theta - \theta_c) \\
& + \frac{1}{\pi R^2} \frac{R^2}{32} [r^2\mathcal{I}_n(R)\mathcal{K}_n(r) \\
& - 2rR\mathcal{I}_{n+1}(R)\mathcal{K}_{n+1}(r) \\
& + R^2\mathcal{I}_{n+2}(R)\mathcal{K}_{n+2}(r)] \cos((n+2)\theta - n\theta_c), \tag{52}
\end{aligned}$$

$$\begin{aligned}
u_{3,1}^{(i)} = & \frac{1}{\pi R^2} \frac{R^2}{384} [R^3\mathcal{K}_{n-3}(R)\mathcal{I}_{n-3}(r) \\
& - 3rR^2\mathcal{K}_{n-2}(R)\mathcal{I}_{n-2}(r) \\
& + 3Rr^2\mathcal{K}_{n-1}(R)\mathcal{I}_{n-1}(r) \\
& - r^3\mathcal{K}_n(R)\mathcal{I}_n(r)] \cos((n-3)\theta + n\theta_c) \\
& + \frac{1}{\pi R^2} \frac{R^2}{128} \left[ -\frac{n+1}{n-1}rR^2\mathcal{K}_{n-2}(R)\mathcal{I}_{n-2}(r) \right. \\
& + R\left(\frac{2(n+1)}{n}r^2 + R^2\right)\mathcal{K}_{n-1}(R)\mathcal{I}_{n-1}(r) \\
& - r\left(r^2 + \frac{2(n-2)}{n-1}R^2\right)\mathcal{K}_n(R)\mathcal{I}_n(r) \\
& \left. + r^2R\frac{n-2}{n}\mathcal{K}_{n+1}(R)\mathcal{I}_{n+1}(r) \right] \\
& \times \cos((n-1)\theta - n\theta_c) \\
& + \frac{1}{\pi R^2} \frac{R^2}{128} \left[ \frac{n+2}{n}r^2R\mathcal{K}_{n-1}(R)\mathcal{I}_{n-1}(r) \right. \\
& - r\left(r^2 + \frac{2(n+2)}{n+1}R^2\right)\mathcal{K}_n(R)\mathcal{I}_n(r) \\
& + R\left(\frac{2(n-1)}{n}r^2 + R^2\right)\mathcal{K}_{n+1}(R)\mathcal{I}_{n+1}(r) \\
& \left. - rR^2\frac{n-1}{n+1}\mathcal{K}_{n+2}(R)\mathcal{I}_{n+2}(r) \right] \\
& \times \cos((n+1)\theta - n\theta_c) \\
& + \frac{1}{\pi R^2} \frac{R^2}{384} [-r^3\mathcal{K}_n(R)\mathcal{I}_n(r) \\
& + 3r^2R\mathcal{K}_{n+1}(R)\mathcal{I}_{n+1}(r) \\
& - 3rR^2\mathcal{K}_{n+2}(R)\mathcal{I}_{n+2}(r) \\
& + R^3\mathcal{K}_{n+3}(R)\mathcal{I}_{n+3}(r)] \cos((n+3)\theta - n\theta_c), \tag{53}
\end{aligned}$$

$$\begin{aligned}
u_{3,1}^{(o)} = & \frac{1}{\pi R^2} \frac{R^2}{384} \left[ R^3 \mathcal{I}_{n-3}(R) \mathcal{K}_{n-3}(r) \right. \\
& - 3rR^2 \mathcal{I}_{n-2}(R) \mathcal{K}_{n-2}(r) \\
& + 3r^2 R \mathcal{I}_{n-1}(R) \mathcal{K}_{n-1}(r) \\
& \left. - r^3 \mathcal{I}_n(R) \mathcal{K}_n(r) \right] \cos((n-3)\theta - n\theta_c) \\
& + \frac{1}{\pi R^2} \frac{R^2}{128} \left[ -\frac{n+1}{n-1} rR^2 \mathcal{I}_{n-2}(R) \mathcal{K}_{n-2}(r) \right. \\
& + R \left( \frac{2(n+1)}{n} r^2 + R^2 \right) \mathcal{I}_{n-1}(R) \mathcal{K}_{n-1}(r) \\
& - r \left( r^2 + \frac{2(n-2)}{n-1} R^2 \right) \mathcal{I}_n(R) \mathcal{K}_n(r) \\
& \left. + \frac{n-2}{n} r^2 R \mathcal{I}_{n+1}(R) \mathcal{K}_{n+1}(r) \right] \\
& \times \cos((n-1)\theta - n\theta_c) \\
& + \frac{1}{\pi R^2} \frac{R^2}{128} \left[ \frac{n+2}{n} r^2 R \mathcal{I}_{n-1}(R) \mathcal{K}_{n-1}(r) \right. \\
& - r \left( r^2 + \frac{2(n+2)}{n+1} R^2 \right) \mathcal{I}_n(R) \mathcal{K}_n(r) \\
& + R \left( \frac{2(n-1)}{n} r^2 + R^2 \right) \mathcal{I}_{n+1}(R) \mathcal{K}_{n+1}(r) \\
& \left. - \frac{n-1}{n+1} rR^2 \mathcal{I}_{n+2}(R) \mathcal{K}_{n+2}(r) \right] \\
& \times \cos((n+1)\theta - n\theta_c) \\
& + \frac{1}{\pi R^2} \frac{R^2}{384} \left[ -r^3 \mathcal{I}_n(R) \mathcal{K}_n(r) \right. \\
& + 3r^2 R \mathcal{I}_{n+1}(R) \mathcal{K}_{n+1}(r) \\
& - 3rR^2 \mathcal{I}_{n+2}(R) \mathcal{K}_{n+2}(r) \\
& \left. + R^3 \mathcal{I}_{n+3}(R) \mathcal{K}_{n+3}(r) \right] \cos((n+3)\theta - n\theta_c). \quad (54)
\end{aligned}$$

Using the above description, the force and torque in Eqs. (15) and (16) are calculated.

In the case of  $n = 2$ , we obtain

$$\begin{aligned}
\mathbf{F}^{(2)} = & \left[ (f_{1,0}^{(2)} - f_{1,1}^{(2)} \epsilon \cos 2\theta_c) \delta \right. \\
& - (f_{3,0}^{(2)} - 2f_{3,1}^{(2)} \epsilon \cos 2\theta_c) \delta^3 \Big] \mathbf{e}_x \\
& - \left[ (f_{1,1}^{(2)} \epsilon \sin 2\theta_c) \delta - (f_{3,1}^{(2)} \epsilon \sin 2\theta_c) \delta^3 \right] \mathbf{e}_y, \quad (55)
\end{aligned}$$

$$N^{(2)} = g_{2,1}^{(2)} \epsilon \delta^2 \sin 2\theta_c, \quad (56)$$

where

$$f_{1,1}^{(2)} = \frac{R^2}{2} [\mathcal{I}_1(R) \mathcal{K}_1(R) - \mathcal{I}_2(R) \mathcal{K}_2(R)], \quad (57)$$

$$\begin{aligned}
f_{3,1}^{(2)} = & \frac{R^4}{96} [3\mathcal{I}_0(R) \mathcal{K}_0(R) - 4\mathcal{I}_1(R) \mathcal{K}_1(R) \\
& + \mathcal{I}_2(R) \mathcal{K}_2(R)], \quad (58)
\end{aligned}$$

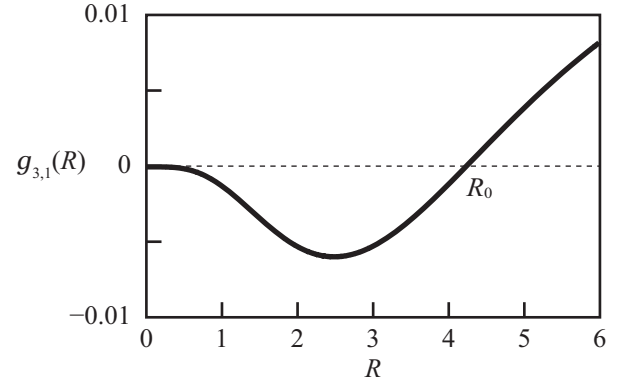


FIG. 1. Plot of the coefficient  $g_{3,1}^{(3)}$  against the particle radius  $R$ . It is positive and negative for  $R > R_0$  and  $R < R_0$ , respectively, where  $R_0 \simeq 4.23024$ .

$$\begin{aligned}
g_{2,1}^{(2)} = & \frac{R^4}{32} [2\mathcal{I}_0(R) \mathcal{K}_0(R) - \mathcal{I}_1(R) \mathcal{K}_1(R) \\
& - 2\mathcal{I}_2(R) \mathcal{K}_2(R) + \mathcal{I}_3(R) \mathcal{K}_3(R)], \quad (59)
\end{aligned}$$

where  $f_{1,1}^{(2)} > 0$ ,  $f_{3,1}^{(2)} > 0$ , and  $g_{2,1}^{(2)} > 0$  for  $\forall R > 0$ .

These results suggest that the force is directed in the  $x$ -axis direction only for  $\theta_c = 0$  or  $\pi/2$  considering that  $\theta_c$  has  $\pi$ -periodicity. In such cases, the bifurcation point for the translational motion is

$$\eta_t = f_{1,0}^{(2)} - \epsilon f_{1,1}^{(2)} \cos 2\theta_c. \quad (60)$$

The maximum bifurcation point for  $\eta_t$  is achieved when  $\cos 2\theta_c = -1$ , that is to say,  $\theta_c = \pi/2$ . Therefore, the bifurcation point for the motion in a minor-axis direction is the greatest. It means that the translational motion is realized for smaller resistance coefficient, that is to say, the elliptic camphor particle tends to move in its minor-axis direction, which is the same as the discussion in our previous papers [18, 24, 25].

From the present results, we can also discuss the torque working on the camphor particle moving at a constant velocity. The torque depends on the characteristic angle  $\theta_c$ , namely the torque is proportional to  $\sin 2\theta_c$ . Considering that the torque is working on an elliptic camphor particle moving in the  $x$ -axis direction if and only if  $\theta_c \neq 0, \pi/2$ , the characteristic angle  $\theta_c$  should be  $\theta_c = 0$  or  $\pi/2$  for the solution with constant  $\theta_c$ . By considering the sign of the torque, it is concluded that the solution with  $\theta_c = 0$  and  $\pi/2$  are unstable and stable, respectively. In other words, the direction of the elliptic camphor particle motion should converge to its minor-axis direction.

Next, we consider the case of  $n = 3$ . We obtain

$$\mathbf{F}^{(3)} = [f_{1,0}^{(3)} \delta - f_{3,0}^{(3)} \delta^3] \mathbf{e}_x, \quad (61)$$

$$N^{(3)} = g_{3,1}^{(3)} \epsilon \delta^3 \sin 3\theta_c, \quad (62)$$

where

$$g_{3,1}^{(3)} = \frac{R^5}{384} [-3\mathcal{I}_0(R)\mathcal{K}_0(R) + 3\mathcal{I}_1(R)\mathcal{K}_1(R) + 2\mathcal{I}_2(R)\mathcal{K}_2(R) - 3\mathcal{I}_3(R)\mathcal{K}_3(R) + \mathcal{I}_4(R)\mathcal{K}_4(R)]. \quad (63)$$

These results suggest that the bifurcation point for the translational motion does not depend on the direction of the particle. However, once the particle begins to move, the torque works on the particle. The direction of the torque depends on the sign of  $g_{3,1}^{(3)}$ . Interestingly, the sign of  $g_{3,1}^{(3)}$  changes depending on the particle radius  $R$ . In Fig. 1, the plot of  $g_{3,1}^{(3)}$  against  $R$  is shown, in which  $g_{3,1}^{(3)}$  is negative and positive and for  $R < R_0$  and  $R > R_0$ , respectively.  $R_0$  is numerically obtained as

$$R_0 \simeq 4.23024. \quad (64)$$

This result suggests that the smaller particle moves in the direction of a corner, a more convex part, while the larger particle in the direction of a side, a flatter part.

#### IV. NUMERICAL CALCULATION

Numerical calculation was performed for the confirmation of theoretical results. Equations (10) to (19) were used for the numerical calculation, though Eqs. (11), (15), and (16) were slightly changed for stable numerical calculation as

$$\Theta(\mathbf{r}; \mathbf{r}_c, \theta_c) = \frac{1}{2} \left[ 1 + \tanh \frac{|\mathbf{r} - \mathbf{r}_c| - F(\phi - \theta_c)}{\Delta w} \right], \quad (65)$$

$$\mathbf{F} = - \int_{\mathbb{R}^2} (\nabla' u(\mathbf{r}')) \Theta(\mathbf{r}'; \mathbf{r}_c, \theta_c) dA', \quad (66)$$

$$N = - \int_{\mathbb{R}^2} \mathbf{r}' \times (\nabla' u(\mathbf{r}')) \Theta(\mathbf{r}'; \mathbf{r}_c, \theta_c) dA', \quad (67)$$

where  $\Delta w$  is a smoothing parameter, and  $\phi$  is the angle of  $\mathbf{r} - \mathbf{r}_c$  from the  $x$ -axis. We changed  $R$  as a parameter. The periodic boundary condition was adopted for the concentration field  $u$ , which was defined in a square with a side of  $20R$ . We used the Euler method for the time development and the explicit method for the spatial derivative. The space and time steps were set to be  $\Delta x = R/40$  and  $\Delta t = 10^{-4} \times R^2$ . The parameters were set as follows:  $m$  and  $I$  were set as

$$m = \rho A = \rho \pi R^2 \left( 1 + \frac{\epsilon^2}{2} \right), \quad (68)$$

$$I = \frac{\rho \pi R^4}{4} \left( 1 + 3\epsilon^2 + \frac{3}{8}\epsilon^4 \right). \quad (69)$$

Here, we set  $\rho = 10^{-3}$ . The friction coefficients for the translational and rotational motions were determined from the theoretical estimation of the bifurcation point for a circular particle; The bifurcation points were calculated as

$$\eta_t^{(bp)} = \frac{R^2}{4} [\mathcal{I}_0(R)\mathcal{K}_0(R) - \mathcal{I}_2(R)\mathcal{K}_2(R)], \quad (70)$$

$$\eta_r^{(bp)} = \frac{\epsilon^2 n R^4}{4} [\mathcal{I}_{n-1}(R)\mathcal{K}_{n-1}(R) - \mathcal{I}_{n+1}(R)\mathcal{K}_{n+1}(R)], \quad (71)$$

and we set

$$\eta_t = 0.9\eta_t^{(bp)}, \quad (72)$$

$$\eta_r = 1.1\eta_r^{(bp)}. \quad (73)$$

The parameter representing the modification amplitude was set as  $\epsilon = 0.1$ .

The results of numerical calculation in the case of the two-mode modification ( $n = 2$ ) are shown in Fig. 2, which shows the snapshots of the camphor concentration field  $u$  together with the particle shape and the motion direction after sufficiently long time. For each  $R$ , the camphor particle moves in its minor-axis direction. In order to clearly show the relation between the direction of motion and shape, the angle difference between the direction of velocity  $\phi_c$  and the characteristic angle  $\theta_c$ :

$$\Delta\theta_c = \theta_c - \phi_c. \quad (74)$$

Here,  $\phi_c$  is defined as

$$\mathbf{v}_c = |\mathbf{v}_c| \begin{pmatrix} \cos \phi_c \\ \sin \phi_c \end{pmatrix}. \quad (75)$$

It should be noted that  $\Delta\theta_c$  is set in the range of

$$-\frac{\pi}{2n} < \Delta\theta_c \leq \frac{3\pi}{2n}, \quad (76)$$

reflecting the  $(2\pi/n)$ -periodicity of  $\theta_c$ . The time evolution of  $\Delta\theta_c$  is shown in Fig. 2(a), which exemplifies that  $\Delta\theta_c$  eventually converged to  $\pi/2$ . This means that the particle moves in its minor-axis direction.

Figure 3 shows the numerical results in the case of the three-mode modification ( $n = 3$ ), which shows the snapshot of the camphor concentration field  $u$  together with the particle shape and the motion direction for each  $R$  after sufficiently long time. In Fig. 3(a), the time evolution of  $\Delta\theta_c$  for  $n = 3$  is plotted for each  $R$ .  $\Delta\theta_c$  converged to 0 for  $R = 1, 2, 3$  and 4, while it converged to  $\pi/3$  for  $R = 5$  and 6. In other words, the triangular camphor particle moved in the direction of a corner for  $R = 1, 2, 3$ , and 4, while it moved in the direction of a side for  $R = 5$  and 6. These results well correspond to the theoretical prediction that a triangular particle moves in the direction of a corner and a side for  $R < R_0$  and  $R > R_0$ , respectively, where  $R_0 \simeq 4.23024$ . Compared with the case of  $n = 2$ , the change in  $\Delta\theta_c$  is slower since the torque is proportional to  $\delta^3$  for  $n = 3$ , while it is proportional to  $\delta^2$  for  $n = 2$ .

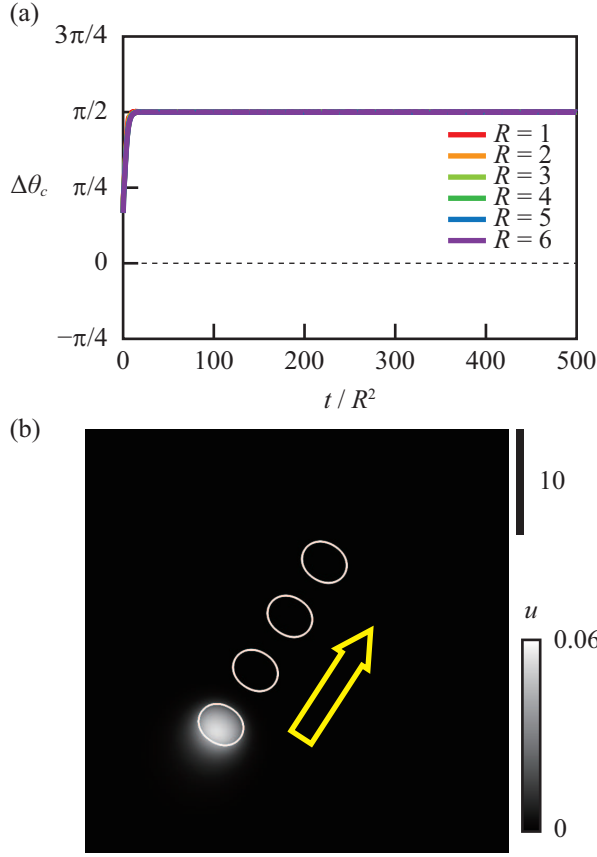


FIG. 2. Numerical results in the case of the two-mode modification. (a) Time series of  $\Delta\theta_c$  for  $R = 1$  (red), 2 (orange), 3 (yellow green), 4 (green), 5 (blue), and 6 (purple).  $\Delta\theta_c$  is plotted against  $t/R^2$ . For all  $R$ ,  $\Delta\theta_c$  is converged to  $\pi/2$ . (b) Concentration field  $u$  for  $R = 2$  after sufficiently long time from the start of simulation. The positions and directions of the camphor particle with a time interval of 20 are shown with the white curves. The direction of motion is indicated with a yellow arrow. A scale bar is shown on the right.

## V. DISCUSSION AND SUMMARY

In the present study, we performed theoretical analyses for the camphor particle motion with an infinitesimally small  $n$ -mode modification from a circle. We calculated the concentration field by the perturbation method up to the third order of velocity  $\delta$  and the first order of the modification amplitude  $\epsilon$ . Based on the calculated concentration field, we obtained the force and torque that work on the particle. In our previous study [18, 24, 25], we could only calculate the force in the case that the velocity is in the direction of either major or minor axis. However, we could not determine the preferable direction for the camphor particle with the three- or higher-mode modification from a circle using the same framework since we did not calculate the torque for the camphor particle exhibiting translational motion. In the present study, we discussed the time evolution of the characteristic angle  $\theta_c$  by calculating the torque for the general configura-

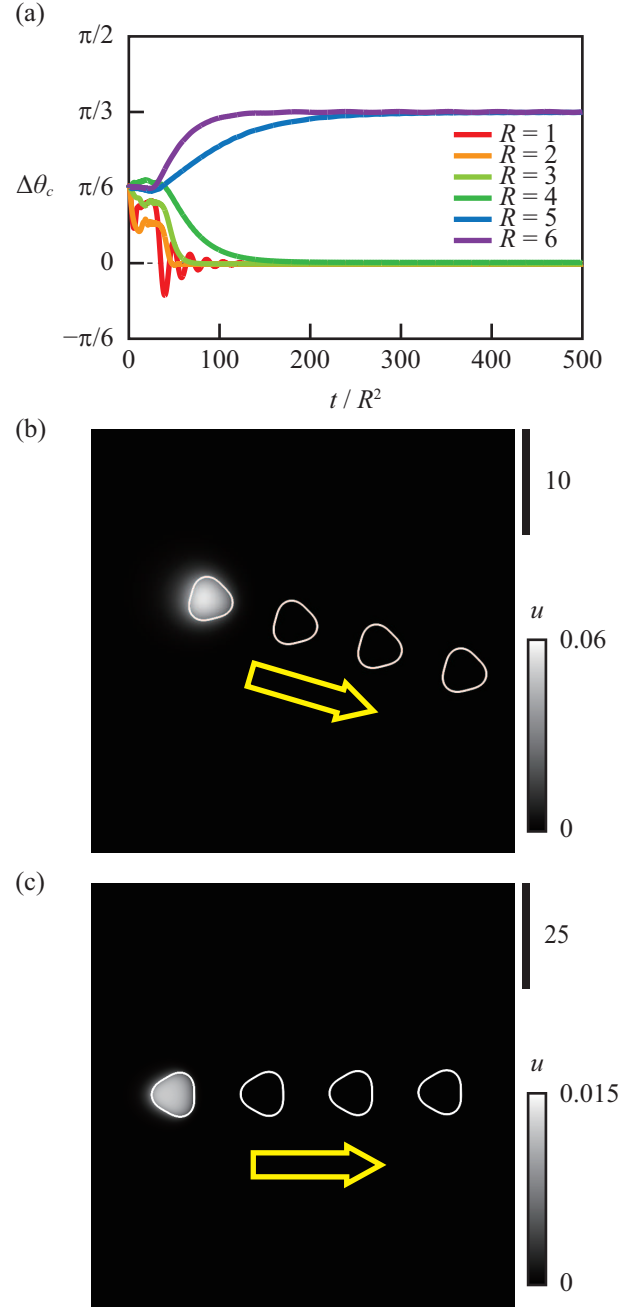


FIG. 3. Numerical results in the case of the three-mode modification. (a) Time series of  $\Delta\theta_c$  for  $R = 1$  (red), 2 (orange), 3 (yellow green), 4 (green), 5 (blue), and 6 (purple).  $\Delta\theta_c$  is plotted against  $t/R^2$ .  $\Delta\theta_c$  is converged to 0 for  $R = 1, 2, 3$ , and 4, while it is converged to  $\pi/3$  for  $R = 5$  and 6. (b,c) Concentration field  $u$  for  $R = 2$  (b) and  $R = 5$  (c) after sufficiently long time from the start of simulation. The positions and directions of the camphor particle with a time interval of 40 (b) and 250 (c) are shown with the white curves. The directions of motion are indicated with yellow arrows. Respective scale bars are shown on the right.



tion, and thus could derive a preferable direction for the camphor particle with the three-mode modification.

For the camphor particle with the modification of  $n \geq 4$  from a circle, we cannot determine the preferable direction by only calculating the concentration field with respect to the third order of the velocity  $\delta$ . It may be possible to calculate it if the concentration field is calculated up to the  $n$ -th order of  $\delta$ , and we expect that the torque is in the order of  $\epsilon\delta^n$ . Considering that the present theory is applicable only in the regime close to the bifurcation point, the term of  $\delta^n$  with larger  $n$  becomes so small that the torque can practically rotate the particle very slowly. In this sense, the discussion for the preferable direction for larger  $n$  might become meaningless.

The motion of a point-like camphor particle confined in a circular region was recently analyzed [38]. It would be interesting to discuss the coupling between the particle shape and boundary shape with respect to the symmetric properties. The interaction among particles has also been studied [39–43]. We discussed the interaction between the two elliptic camphor particles whose center positions are fixed [44]. As a natural extension of these previous studies, the dynamics of the mobile particles that interact with each other depending on their characteristic direction, like a nematic interaction, is an interesting problem. Using a multiple-camphor-particle system with the modification from a circle, we believe we can realize such a system.

It is also known that a pentanol droplet on the almost saturated pentanol aqueous solution spontaneously moves with a banana-like-shaped deformation [26]. The mechanism of the motion is almost the same as the one for a camphor particle at the water surface. Other systems with moving droplets with deformation, which are driven by the surface tension gradient, have also been reported [5, 29–31]. In the present study, we establish how to calculate the effect of the shape on the motion. For the droplet system, the motion can affect the deformation, and thus the motion and deformation are coupled with each other. The present work can be further extended to the study for clarifying the mechanism of the coupling between motion and deformation.

## ACKNOWLEDGMENTS

The authors acknowledge Masaharu Nagayama and Yutaka Sumino for their helpful discussion. This work was supported by JSPS KAKENHI Grant Nos. JP16H03949, JP19K03765, and JP19J00365, and the Cooperative Research Program of “Network Joint Research Center for Materials and Devices” (Nos. 20194006, and 20191030). This work was also supported by JSPS and PAN under the Japan-Poland Research Cooperative Program “Spatio-temporal patterns of elements driven by self-generated, geometrically constrained flows”.

## Appendix A: calculation of Eqs. (7) and (8)

Here, we derive the last description in Eqs. (7) and (8). We set the polar coordinates  $(r', \theta')$ , so that the arbitrary position  $\mathbf{r}'$  is described as

$$\mathbf{r}' = \mathbf{q}(\theta') = R[1 + F(\theta')] \mathbf{e}(\theta'), \quad (\text{A1})$$

where  $\mathbf{e}(\theta')$  is a unit vector in the direction of  $\theta'$ . For the force in Eq. (7), we obtain

$$\begin{aligned} F_i &= \int_{\partial\Omega(\mathbf{r}_c, \theta_c)} \gamma(u(\mathbf{r}')) n_i(\mathbf{r}') d\ell' \\ &= \int_0^{2\pi} \gamma(u(\mathbf{q}(\theta'))) \varepsilon_{ij} \frac{dq_j}{d\theta'} d\theta' \\ &= [\gamma(u(\mathbf{q}(\theta))) \varepsilon_{ij} q_j(\theta)]_0^{2\pi} \\ &\quad - \int_0^{2\pi} \left( \frac{d}{d\theta'} \gamma(u(\mathbf{q}(\theta'))) \right) \varepsilon_{ij} q_j(\theta') d\theta' \\ &= - \int_0^{2\pi} \frac{\partial \gamma}{\partial q_k} \frac{dq_k}{d\theta'} \varepsilon_{ij} q_j(\theta') d\theta' \\ &= - \int_{\partial\Omega(\mathbf{r}_c, \theta_c)} \frac{\partial \gamma}{\partial q_k} \varepsilon_{ij} q_j dq_k \\ &= - \iint_{\Omega(\mathbf{r}_c, \theta_c)} \varepsilon_{mk} \frac{\partial}{\partial r'_m} \left( \frac{\partial \gamma}{\partial r'_k} \varepsilon_{ij} r'_j \right) dA' \\ &= - \iint_{\Omega(\mathbf{r}_c, \theta_c)} \varepsilon_{ij} \varepsilon_{jk} \frac{\partial \gamma}{\partial r'_k} dA' \\ &= \iint_{\Omega(\mathbf{r}_c, \theta_c)} \frac{\partial \gamma}{\partial r'_i} dA' \\ &= \iint_{\Omega(\mathbf{r}_c, \theta_c)} [\nabla' \gamma]_i dA'. \end{aligned} \quad (\text{A2})$$

The Green’s theorem is used in the calculation, and  $\varepsilon_{ij}$  is set as

$$\varepsilon_{ij} = \begin{cases} 1, & i = 1, j = 2, \\ -1, & i = 2, j = 1, \\ 0, & i = j, \end{cases} \quad (\text{A3})$$

where it should be noted that

$$\varepsilon_{ij} \varepsilon_{jk} = -\delta_{ik}, \quad (\text{A4})$$

and

$$\mathbf{a} \times \mathbf{b} = \varepsilon_{ij} a_i b_j \quad (\text{A5})$$

hold. Here,  $\delta_{ij}$  is the Kronecker's delta. For the torque in Eq. (8), we obtain

$$\begin{aligned}
N &= \int_{\partial\Omega(\mathbf{r}_c, \theta_c)} (\mathbf{r}' - \mathbf{r}_c) \times \gamma(u(\mathbf{r}')) \mathbf{n}(\mathbf{r}') d\ell' \\
&= \int_{\partial\Omega(\mathbf{r}_c, \theta_c)} \varepsilon_{ij} (r'_i - r_{c,i}) \gamma(u(\mathbf{r}')) n_j(\mathbf{r}') d\ell' \\
&= \int_0^{2\pi} \gamma(u(\mathbf{q}(\theta'))) \varepsilon_{ij} (q_i(\theta') - r_{c,i}) \varepsilon_{jk} \frac{dq_k}{d\theta'} d\theta' \\
&= - \int_0^{2\pi} \gamma(u(\mathbf{q}(\theta'))) (q_i(\theta') - r_{c,i}) \frac{dq_i}{d\theta'} d\theta' \\
&= - \int_{\partial\Omega(\mathbf{r}_c, \theta_c)} \gamma(u(\mathbf{q})) (q_i - r_{c,i}) dq_i \\
&= - \iint_{\Omega(\mathbf{r}_c, \theta_c)} \varepsilon_{mi} \frac{\partial}{\partial r'_m} (\gamma(u(\mathbf{r}')) (r'_i - r_{c,i})) dA' \\
&= \iint_{\Omega(\mathbf{r}_c, \theta_c)} \varepsilon_{mi} (r'_i - r_{c,i}) \frac{\partial \gamma}{\partial r'_m} dA' \\
&= \iint_{\Omega(\mathbf{r}_c, \theta_c)} [(\mathbf{r}' - \mathbf{r}_c) \times \nabla' \gamma] dA'. \tag{A6}
\end{aligned}$$

- 
- [1] S. Ramaswamy, *Annu. Rev. Cond. Mat. Phys.* **1**, 323 (2010).
- [2] T. Ohta, *J. Phys. Soc. Jpn.* **86**, 072001 (2017).
- [3] M. C. Marchetti, J. F. Joanny, S. Ramaswamy, T. B. Liverpool, J. Prost, M. Rao, and R. A. Simha, *Rev. Mod. Phys.* **85**, 1143 (2013).
- [4] C. Bechinger, R. Di Leonardo, H. Löwen, C. Reichhardt, G. Volpe, and G. Volpe, *Rev. Mod. Phys.* **88**, 045006 (2016).
- [5] V. Pimienta and C. Antoine, *Curr. Opin. Colloid Interface Sci.* **19**, 290 (2014).
- [6] K. Keren, Z. Pincus, G. M. Allen, E. L. Barnhart, G. Marriott, A. Mogilner, and J. A. Theriot, *Nature* **453**, 475 (2008).
- [7] T. Ohta and T. Ohkuma, *Phys. Rev. Lett.* **102**, 154101 (2009).
- [8] H. Ebata and M. Sano, *Sci. Rep.* **5**, 8546 (2015).
- [9] H. Ebata, A. Yamamoto, Y. Tsuji, S. Sasaki, K. Moriyama, T. Kuboki, and S. Kidoaki, *Sci. Rep.* **8**, 5153 (2018).
- [10] W. Skey, *Trans. Proc. R. Soc. New Zealand* **11**, 473 (1878).
- [11] C. Tomlinson, *Proc. R. Soc. London* **11**, 575 (1862).
- [12] L. Rayleigh, *Proc. R. Soc. London* **47**, 364 (1889).
- [13] S. Nakata, Y. Iguchi, S. Ose, M. Kuboyama, T. Ishii, and K. Yoshikawa, *Langmuir* **13**, 4454 (1997).
- [14] Y. Hayashima, M. Nagayama, and S. Nakata, *J. Phys. Chem. B* **105**, 5353 (2001).
- [15] X. Chen, S.-I. Ei, and M. Mimura, *Netw. Heterog. Media* **4**, 1 (2009).
- [16] M. Nagayama, S. Nakata, Y. Doi, and Y. Hayashima, *Physica D* **194**, 151 (2004).
- [17] S. Nakata, M. Nagayama, H. Kitahata, N. J. Suematsu, and T. Hasegawa, *Phys. Chem. Chem. Phys.* **17**, 10326 (2015).
- [18] H. Kitahata, Y. Koyano, K. Iida, and M. Nagayama, in *Self-organized motion: Physicochemical design based on nonlinear dynamics*, eds. S. Nakata, V. Pimienta, I. Lagzi, H. Kitahata, and N. J. Suematsu (R. Soc. Chem., Cambridge, 2019).
- [19] H. Morohashi, M. Imai, and T. Toyota, *Chem. Phys. Lett.* **721**, 104 (2019).
- [20] S. Nakata, K. Kayahara, M. Kuze, E. Ginder, M. Nagayama, and H. Nishimori, *Soft Matter* **14**, 3791 (2018).
- [21] Y. Koyano, M. Gryciuk, P. Skrobanska, M. Malecki, Y. Sumino, H. Kitahata, and J. Gorecki, *Phys. Rev. E* **96**, 012609 (2017).
- [22] Y. Koyano, H. Kitahata, M. Gryciuk, N. Akulich, A. Gorecka, M. Malecki, and J. Gorecki, *Chaos* **29**, 013125 (2019).
- [23] J. Sharma, I. Tiwari, D. Das, P. Parmananda, V. S. Akella, and V. Pimienta, *Phys. Rev. E* **99**, 012204 (2019).
- [24] H. Kitahata, K. Iida, and M. Nagayama, *Phys. Rev. E* **87**, 010901 (2013).
- [25] K. Iida, H. Kitahata, and M. Nagayama, *Physica D* **272**, 39 (2014).
- [26] K. Nagai, Y. Sumino, H. Kitahata, and K. Yoshikawa, *Phys. Rev. E* **71**, 065301 (2005).
- [27] Y. Sumino, N. Magome, T. Hamada, and K. Yoshikawa, *Phys. Rev. Lett.* **94**, 068301 (2005).
- [28] T. Bansagi Jr., M. M. Wrobel, S. K. Scott, and A. F. Taylor, *J. Phys. Chem. B* **117**, 13572 (2013).
- [29] V. Pimienta, M. Brost, N. Kovalchuk, S. Bresch, and O. Steinbock, *Angew. Chem., Int. Ed.* **50**, 10728 (2011).
- [30] I. Lagzi, S. Soh, P. J. Wesson, K. P. Browne, and B. A. Grzybowski, *J. Am. Chem. Soc.* **132**, 1198 (2010).
- [31] J. Čejková, F. Štěpánek, and M. M. Hanczyc, *Langmuir* **32**, 4800 (2016).

- [32] A. G. Vecchiarelli, K. C. Neuman, and K. Mizuuchi, *Proc. Natl. Acad. Sci. (U.S.A.)* **111**, 4880 (2014).
- [33] E. J. Banigan and J. F. Marko, *Phys. Rev. E* **93**, 012611 (2016).
- [34] N. J. Suematsu, T. Sasaki, S. Nakata, and H. Kitahata, *Langmuir* **30**, 8101 (2014).
- [35] H. Kitahata and N. Yoshinaga, *J. Chem. Phys.* **148**, 134906 (2018).
- [36] T. Bickel, *Soft Matter* **15**, 3644 (2019).
- [37] C. C. de Wit and R. F. Makens, *J. Am. Chem. Soc.* **54**, 455 (1932).
- [38] Y. Koyano, N. J. Suematsu, and H. Kitahata, *Phys. Rev. E* **99**, 022211 (2019).
- [39] S. Soh, K. J. M. Bishop, and B. A. Grzybowski, *J. Phys. Chem. B* **112**, 10848 (2008).
- [40] S. Soh, M. Branicki, and B. A. Grzybowski, *J. Phys. Chem. Lett.* **2**, 770 (2011).
- [41] N. J. Suematsu, K. Tateno, S. Nakata, and H. Nishimori, *J. Phys. Soc. Jpn.* **84**, 034802 (2015).
- [42] H. Nishimori, N. J. Suematsu, and S. Nakata, *J. Phys. Soc. Jpn.* **86**, 101012 (2017).
- [43] Y. Matsuda, K. Ikeda, Y. Ikura, H. Nishimori, and N. J. Suematsu, *J. Phys. Soc. Jpn.* **88**, 093002 (2019).
- [44] S.-I. Ei, H. Kitahata, Y. Koyano, and M. Nagayama, *Physica D* **366**, 10 (2018).